

## The Scattering of Protons by Tritons

R. S. CLAASSEN, R. J. S. BROWN, G. D. FREIER, AND W. R. STRATTON  
*Department of Physics, University of Minnesota, Minneapolis, Minnesota*  
 (Received February 16, 1951)

The differential cross section for the scattering of protons by tritons has been measured in the angular range of  $41.85^\circ$  to  $163^\circ$  in the laboratory ( $54.7^\circ$  to  $168.7^\circ$  in the center-of-mass system) at five energies between 2.54 and 3.50 Mev using protons from the Minnesota electrostatic generator. A small volume (42 cc) scattering chamber with an angular range of  $17^\circ$  to  $163^\circ$  was used for these measurements. Measurements of proton-proton and proton-helium cross sections and a comparison of the results with those obtained previously with a large scattering chamber showed that this small chamber gave results too high (about 3 percent) at the low scattering angles. These measurements determined a correction which was applied in the calculation of the  $p$ - $T$  cross sections from the experimental data. The center-of-mass differential cross section varies between a maximum of  $0.243 \times 10^{-24}$  cm<sup>2</sup> per unit solid angle at  $54.7^\circ$  and 3.5 Mev and a minimum of  $0.065 \times 10^{-24}$  cm<sup>2</sup> per unit solid angle at  $109.5^\circ$  and 3.5 Mev in the angle and energy range studied. The cross sections considered as a function of angle display a strong minimum, near  $100^\circ$ , in the center-of-mass coordinate system. The cross section for a given angle is a slowly varying function of energy.

### I. INTRODUCTION

A GREAT deal of the present theory of nuclear forces is based on quantitative information obtained from experiments in which a detailed study is made of the scattering of protons from light nuclei. The problem reported here is part of a general program of study of the matrix of interactions among all of the light nuclei. Careful work has been done on the measurement of the differential cross section for the scattering of protons by protons,<sup>1-3</sup> protons by deuterons,<sup>4</sup> and protons by helium.<sup>5</sup> While several authors have shown that the  $p$ - $p$  data can be fitted by an  $S$ -wave phase shift analysis,<sup>6-8</sup> the  $p$ - $d$  and  $p$ -He data require addition of states of higher angular momentum to account for the scattering from these nuclei of greater spatial extent.<sup>9,10</sup>

Hemmendinger, Jarvis, and Taschek<sup>11,12</sup> have adapted the techniques of scattering measurements to utilize small gas sample targets and have measured the cross section for the scattering of protons by tritons over the energy range available with the 2.5-Mev van de graaff generator at Los Alamos. Although the data obtained by them has not yet been analyzed by the phase shift

method, it is apparent from their results that there is a strong nuclear interaction between the proton and triton, and, in particular, an interaction in states of angular momentum greater than zero. It was felt that it would be worthwhile to extend these measurements to the higher energy (3.5 Mev) available with the Minnesota generator and to lower and higher scattering angles, where the effects of the higher angular momentum states would be more pronounced.

### II. APPARATUS

Figure 1 shows the essential features of the scattering chamber designed to utilize small gas samples as targets in the study of the angular distribution of the scattered particles and charged reaction products from nuclear collisions. This chamber is similar to the one used by Taschek *et al.*,<sup>13</sup> in that it is a nonplanar chamber; that is, the locus of directions at which scattering can be detected traces out a cone whose vertex is crossed by the incident beam of protons and whose axis is per-

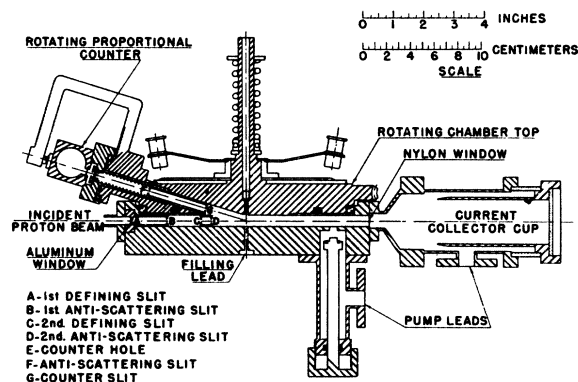


FIG. 1. View of the scattering chamber. The figure is of a plane through the center of the chamber and is drawn with the chamber set for a scattering angle of  $163^\circ$ , the maximum scattering angle for this chamber.

<sup>1</sup> Tuve, Heydenburg, and Hafstad, Phys. Rev. **50**, 806 (1936); Hafstad, Heydenburg, and Tuve, Phys. Rev. **53**, 239 (1938); Heydenburg, Hafstad, and Tuve, Phys. Rev. **56**, 1078 (1939).

<sup>2</sup> Herb, Kerst, Parkinson, and Plain, Phys. Rev. **55**, 998 (1939).

<sup>3</sup> Blair, Freier, Lampi, Sleator, and Williams, Phys. Rev. **74**, 553 (1948).

<sup>4</sup> Sherr, Blair, Kratz, Bailey, and Taschek, Phys. Rev. **72**, 662 (1947).

<sup>5</sup> Freier, Lampi, Sleator, and Williams, Phys. Rev. **75**, 1345 (1949).

<sup>6</sup> Breit, Condon, and Present, Phys. Rev. **50**, 825 (1936); Breit, Thaxton, and Eisenbud, Phys. Rev. **55**, 1018 (1939).

<sup>7</sup> C. L. Critchfield and D. C. Dodder, Phys. Rev. **75**, 419 (1949).

<sup>8</sup> J. D. Jackson and J. M. Blatt, Revs. Modern Phys. **22**, 77 (1950).

<sup>9</sup> C. L. Critchfield, Phys. Rev. **73**, 1 (1948).

<sup>10</sup> C. L. Critchfield and D. C. Dodder, Phys. Rev. **76**, 602 (1949).

<sup>11</sup> Taschek, Jarvis, Hemmendinger, Everhart, and Gittings, Phys. Rev. **75**, 1361 (1949).

<sup>12</sup> Hemmendinger, Jarvis, and Taschek, Phys. Rev. **76**, 1137 (1949).

<sup>13</sup> R. F. Taschek, Rev. Sci. Instr. **19**, 591 (1948).

pendicular to the incident beam. If  $\phi$  denotes the angle of rotation about this axis,  $\alpha$  is the angle of the cone, and  $\theta$  is the desired scattering angle, then

$$\cos\theta = \sin\alpha \cos\phi \quad (1)$$

provided that the zero of  $\phi$  is chosen at the minimum scattering angle.

The solid angle subtended by the counter and the scattering volume are defined by means of a counter slit and counter hole. To maintain good geometry it is necessary to rotate the counter-defining slits about the direction of scattered particles in such a manner that the length of the slit will be perpendicular to the plane formed by the incident and scattered beams. If  $\omega$  is the angle of rotation of the counter slits, and is taken to be zero at the minimum scattering angle, then

$$\cos\omega = \frac{\cos\alpha \cos\phi}{(1 - \sin^2\alpha \cos^2\phi)^{1/2}} \quad (2)$$

The scattering chamber used in this work was constructed with  $\alpha = 73^\circ$ . To obtain a given scattering angle  $\theta$ , the angle  $\phi$  was set to the nearest minute of arc by means of a vernier scale. The true zero for this scale was determined with the aid of mandrils and precision indicators. The angle  $\omega$  was set to the nearest degree by means of an angular scale mounted on the arm holding the proportional counter.

The chamber was constructed of stainless steel. Figure 1 is a plane view of a section through the center of the chamber, drawn with the counter set at the maximum scattering angle. In order to provide accurate positioning of the upper piece as it was rotated with respect to the main body of the chamber, a circle, seven inches in diameter, of precision ball bearings was provided, running between hardened steel inserts. The side thrust of these bearings accurately centered the top piece as it rotated. The moving vacuum seal was made by a  $4\frac{1}{2}$ -in. diameter "O" ring shown in solid black.

The counter-defining slit was mounted in a tube and is shown at G in Fig. 1. The mounting tube was coupled to the proportional counter so that the correct position of  $\omega$  could be set by rotating the entire counter assembly. The moving vacuum seal was made by an "O" ring shown in black in the drawing. The correct position of the counter hole at E was determined by a set of ball bearings outside the "O" ring. The lightly greased rubber "O" rings were tight to a helium leak detector under static conditions and admitted a negligible amount of gas upon rotation of the chamber or counter.

The angle  $\alpha$ , designed to be  $73^\circ$ , was measured on the assembled chamber and found to be  $73^\circ \pm 40''$ , and has been taken to be exactly  $73^\circ$  in all calculations. Mandrils and traveling microscopes were used to make certain that the axis of rotation of the upper chamber passed through the center line of the incident beam hole.

The beam of protons traversing the chamber was defined by slits shown at A and C. The diameter of the

hole at A was 0.1079 cm, of that at C, 0.1187 cm. These holes were 5.87 cm apart, allowing a divergence of  $1.1^\circ$  half-angle. The diameter of the defined beam at the exit window was 0.73 cm, and the diameter of the exit window was 0.95 cm. The holes at B (0.1185-cm diam) and at D (0.172-cm diam) prevented the majority of protons scattered from the slit edges from entering the scattering volume.

The counter slit system, which defined the solid angle subtended by the counter and the region from which particles could be scattered into the counter, consisted of a round hole of area  $A$  at a distance  $R$  from the center of the scattering region and a slit of width  $2b$  at a distance  $R-h$  from the center. (The hole is at E, the slit at G, in Fig. 1.) The slit width  $2b$  was measured on a comparator and found to have an average value of 0.1752 cm, with a  $\frac{1}{2}$  percent variation over the length of the slit. The diameter of the hole as measured on the comparator was 0.3570 cm, giving an area of 0.1010 cm<sup>2</sup>. The distances  $h$  and  $R$  were measured with the aid of mandrils and were found to be 10.038 and 13.670 cm, respectively. The above dimensions, which enter into the calculation of the cross section, are combined into a geometrical constant  $G = 2bA/Rh$ . The above values give  $G = 1.278 \times 10^{-4}$  cm.

The beam of protons from the generator entered the scattering chamber through a 0.15-mil Al window and passed out the opposite side, through a 0.5-mil Nylon window, into a faraday cup. Loss of secondary electron charge from the cup was prevented by electrostatic bias and a transverse magnetic field. The charge collected during a run was stored on a polystyrene condenser. The condenser was discharged through a ballistic galvanometer at the end of a run. The galvanometer was calibrated in place with a L and N standard 0.50 microfarad condenser and a Wolff potentiometer. The calibration was checked periodically during the course of the experiment.

The particles which were scattered through the counter collimating slits and passed through the 0.15-mil Al counter window were detected by a proportional counter filled with an argon-methane mixture. The pulses from the counter were amplified by a preamplifier and amplifier of Los Alamos design<sup>14</sup> (Model 100) equipped with a delay line pulse shaper. The pulses were sorted according to size and counted by a 10-channel differential discriminator, also of Los Alamos design.<sup>15</sup> A slight change in design of the bias circuit made it possible to shift the position of the 5-volt channels in one-volt steps so that the distribution of counts with pulse height could be studied in greater detail. A sliding pulser was used to adjust for equal channel widths to within a few percent.

The presence of hydrogen contamination in the tritium necessitated dealing with a two component target gas system. Since exchange may take place

<sup>14</sup> W. C. Elmore and M. Sands, *Electronics*, 166 (1949).

<sup>15</sup> Reference 14, p. 241.

between the tritium and the hydrogen absorbed by the walls of the containing vessels, this experiment depended upon an ability to measure the tritium concentration in the chamber. The Los Alamos group has shown that it is possible to measure the hydrogen contamination in the course of the scattering experiment itself.<sup>11,12</sup> A proton suffering an elastic collision loses a fraction of its energy depending upon the angle of scattering and the mass of the scattering center. Since the size of the pulse from a proportional counter varies with the energy of the proton traversing it, it is possible to find an angle and energy at which protons scattered from atoms of different masses will be resolved. In the energy range of 2.5 to 3.5 Mev for the incident protons, scattering angles of 45 to 50 degrees gave good resolution of the two proton groups. Figure 2 shows the pulse distribution owing to protons scattered from tritium and from hydrogen contamination. This graph is a plot of five separate runs. After each run the voltage level of the discriminators was raised one volt, which shifted the center of each channel by one volt. The number of counts in each channel was normalized to unit total pressure and unit charge and was plotted at the voltage at the center of that channel.

Measurements were taken only at angles and energies where the particles passed completely through the counter or were stopped completely in the counter window. This assured a clearly defined pulse distribution. The pulses registered in the lower channels in Fig. 2 are from protons scattered from tritons. The second group of pulses arise from the protons scattered from proton contamination. For angles of 50 degrees or less and energies of 2.5 Mev or greater, the recoil tritons had sufficient energy to penetrate the counter window and pass through the counter. These recoil tritons gave rise to large pulses which were generally registered in the surplus channel of the differential discriminator.

From the number of counts in the proton-proton peak, the known geometry of the chamber, and the known  $p$ - $p$  cross section,<sup>2,3</sup> the effective hydrogen pressure can be calculated. The remaining partial pressure is then that of the tritium.

The tritium gas was stored in the form of uranium hydride in a uranium furnace and transferred to the scattering chamber by a handling system of the type designed at Los Alamos.<sup>11</sup> Figure 3 is a schematic diagram of the handling system. The uranium was contained in a quartz envelope, while the rest of the system was constructed of Pyrex glass. A section of  $\frac{1}{8}$ -in. stainless steel tubing, maintained at approximately  $-35^{\circ}\text{C}$  by a mechanical refrigerator, prevented the mercury vapor from entering the scattering chamber. The Toepler pump arrangement provided for efficient transfer of a small quantity of gas from the storage furnace to the chamber.

About five grams of uranium foil were used in the furnace. A pure deuterium sample stored in and

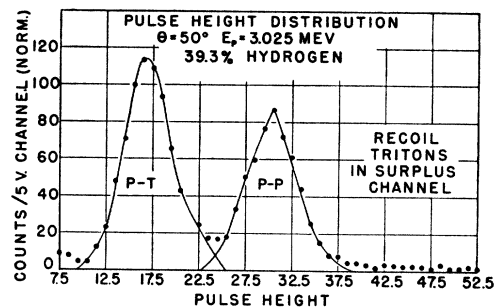


FIG. 2. Pulse-height distribution for protons of 3.03-Mev incident energy scattered at  $50^{\circ}$  from tritium contaminated with hydrogen. The number of counts per 5 volt channel has been normalized to unit charge and pressure and plotted at the voltage at the center of the channel. The pulses caused by recoil tritons were greater than 55 volts and were recorded in the surplus channel.

evolved from this furnace was analyzed for us on a mass spectrometer by Dr. A. O. C. Nier's group. It had acquired a negligible normal hydrogen impurity. Alternate use of the furnace for hydrogen and deuterium showed no "memory" of the previous gas.

The tritium was obtained from the Radioisotopes Division of the Atomic Energy Commission. Each sample provided sufficient gas to fill the scattering chamber to a pressure of 18 mm of Hg, the normal target pressure used in this experiment. During the course of the experiment, the concentration of hydrogen in the tritium sample rose steadily. This was not due primarily to exchange of tritium with hydrogen in the materials of the chamber, as was found by the Los Alamos group,<sup>11</sup>

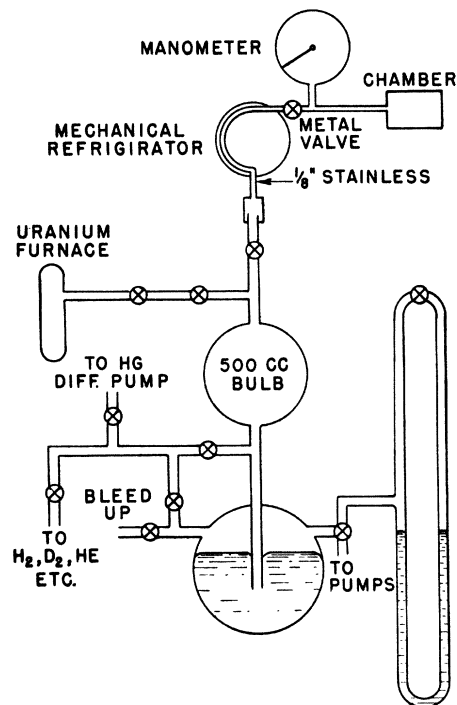


FIG. 3. A schematic diagram of the storage and handling system for the tritium gas.

since a rough calculation showed no appreciable loss of tritium. The total amount of gas rose steadily. This may have been due to hydrogen being released from the walls of the chamber and connecting system or from the decomposition of water vapor or hydrocarbons. Uranium will decompose water, forming uranium oxide, and releasing the hydrogen at elevated temperatures.<sup>16</sup> (During the course of a run, the furnace was exposed to three stopcocks sealed with hydrocarbon grease, which may contribute hydrogen. An attempt was made to use a fluorocarbon grease as a stopcock lubricant, but it proved impractical for vacuum work.)

When a tritium sample became diluted to less than 35 percent tritium, it was removed from the furnace and stored for other work, and a fresh sample was transferred to the furnace.

The pressure of the gas in the chamber was measured by means of a Wallace and Tiernan differential manometer, Model 191. The gauge was calibrated frequently against an oil manometer using Apiezon B oil. After the first weeks of use the calibration settled down and held constant to within 0.02 mm Hg. The gauge was altered for us by the Wallace and Tiernan Company to present only metal surfaces to the gas and was leak tight to a helium leak detector. This gauge proved to be rugged and satisfactory in every respect.

The voltage of the electrostatic generator was controlled and measured by an electrostatic analyzer. The known  $\text{Li}^7(p,n)$  threshold<sup>17</sup> was used to calibrate the voltage scale and to measure the voltage thickness of the entrance window. A lithium fluoride target was placed in the collector cup and the neutron threshold determined with the entrance and exit windows removed. The entrance window was then replaced in the chamber and the threshold was again measured. The apparent shift of the threshold to a higher energy when the window was in place was taken to be the proton energy loss in the entrance window at the threshold energy. The energy loss at other incident energies was calculated, using the curves given in Livingston and Bethe.<sup>18</sup> The energy lost in the gas between the entrance window and the center of the scattering volume was calculated from data given in their article.<sup>18</sup>

The neutron yield was low because of the small collimating slits and resultant low beam currents. For this reason the window thickness determinations were uncertain by  $\pm 10$  kev in the energy region used. Because of this uncertainty, generator instability, and the possibility of a carbon deposit on the input window, an uncertainty of  $\pm 25$  kev has been assigned to the incident proton energy.

### III. PROCEDURE

When not in use, the chamber was maintained at a vacuum of  $3 \times 10^{-6}$  mm of Hg or better by means of an oil diffusion pump and liquid air trap. A gas sample evolved from the uranium furnace into the chamber was used for about four hours, after which time it was returned to the uranium for purification.

Immediately after the chamber was filled, the concentration of the gas sample was determined by a run at  $45^\circ$  or  $50^\circ$ . The concentration determination was then used in the calculations for the runs taken with this filling at other angles where the  $p$ - $p$  protons could not enter the counter or were not resolved from the  $p$ - $l$  protons.

The cross section for scattering at the angle  $\theta$  is given by

$$\sigma(\theta) = (Y \sin \theta) / (qNnG), \quad (3)$$

where  $Y$  is the number of protons counted for charge  $q$ , in microcoulombs, of protons which passed through the chamber.  $N$  is the number of protons in a microcoulomb, taken to be  $6.025 \times 10^{12}$ ;  $n$  is the number of nuclei per  $\text{cm}^3$  at the target temperature and pressure. ( $n$  was calculated by assuming that there are  $6.023 \times 10^{23}$  molecules in  $22,412 \text{ cm}^3$  at S.T.P.) The geometry factor has been defined in Sec. II.

In a two-component target system, there will be a yield  $Y_1$  associated with  $n_1$  target nuclei per  $\text{cm}^3$  (protons) and a yield  $Y_2$  associated with  $n_2$  target nuclei per  $\text{cm}^3$  (tritons). Since  $\sigma(\theta)$  is known for the first process, Eq. (3) may be solved for  $n_1$ . This, together with a measurement of the total pressure, determined  $n_2$ .

The cross section at each angle and energy was measured at least twice, once on each side of the chamber, to reduce any possible asymmetry and reduce the chance of gross errors. Whenever the agreement between measurements was poor, the cross section was remeasured.

### IV. TESTING THE CHAMBER

The scattering chamber was checked against the published proton-proton results<sup>2,3</sup> and the proton-helium results.<sup>5</sup> In the process of testing and checking the performance of the chamber, it became apparent that the results were not valid at all angles and energies, the results being high at the lower scattering angles. As explained later, this was attributed to the small volume of the chamber and the resultant close spacing of the walls of the chamber to the incident beam and to the scattering region. Since the error at a given angle and energy was not the same for different nuclear processes, it was necessary to run check measurements over a range of angles and energies with several nuclear scattering processes whose cross sections were known accurately from previous researches.<sup>2,3,5</sup>

The various experimental quantities which enter into the calculation of the cross section, and which might introduce such an error as was found, were rechecked

<sup>16</sup> F. H. Spedding, *et al.*, *Nucleonics* **4**, 4 (1949).

<sup>17</sup> Herb, Snowdon, and Sala, *Phys. Rev.* **75**, 246 (1949).

<sup>18</sup> M. S. Livingston and H. A. Bethe, *Revs. Modern Phys.* **9**, 270 (1937).

in the course of this testing. The scattering angle  $\theta$  was determined from the geometry of the chamber, the measurement of which has been described in Sec. II. Further, to account for the  $p$ -He results at 2.5 Mev and  $30^\circ$ ,  $\theta$  would have to be in error by  $5^\circ$  ( $\theta$  too small), while to account for the  $p$ -p results at this angle and energy,  $\theta$  would have to be in error by  $12^\circ$  ( $\theta$  too small).

Coulomb scattering from gas impurities could lead to erroneous results at low angles. The helium was shown to have negligible impurity. To eliminate the possibility that Hg vapor from the loading system should contaminate the chamber gas, a liquid air trap was connected directly in front of the exit window. Successive runs with and without cooling of this trap gave the same results within the statistical errors.

At angles above  $20^\circ$ , direct scattering from metal surfaces into the counter contributed a negligible background, as shown by runs taken with the chamber open to the vacuum pumps.

Incorrect energy of the incident protons might give errors which increase with smaller angles and vary with the target gas. The energy of the incident protons was determined by the method described in Sec. II. Furthermore, since both the  $p$ -p and  $p$ -He cross sections considered as a function of energy have both positive and negative slopes in the energy range under investigation, it was possible to eliminate the possibility that incorrect energy, or an energy spread owing to non-uniform windows, is the sole source of our errors.

Second-order geometry corrections,<sup>7</sup> which account for the finite extent of the incident and scattered beams and the resultant spread in angles, amounted to 1 percent or less for angles of  $30^\circ$  or greater in the energy range investigated.

When the cross section of a single gas in the chamber was measured, the curve of the number of proportional counter pulses per voltage interval *versus* pulse height displayed a sharp peak with a long, low tail (see Fig. 4). It was found that, by extrapolating the sharp peak to the base line, consistent results could be obtained for the yield at a given angle and energy. The discarded tail contained from 4 to 7 percent of the yield in the angular range of 45 to 60 degrees and the energy range of 2 to 3.5 Mev.

The tail of the pulse-height curve (Fig. 4) was attributed to protons which had suffered successive collisions with a gas atom and with the metal of the chamber walls or slits, thereby losing more energy than the correctly scattered protons. At low angles this tail was more pronounced (see Fig. 5), and apparently extended back into the proper proton peak far enough to make the measured yield too high. One might expect that these spurious counts were caused by protons which suffered scattering in the gas at small angles where the cross section is high. Since the low angle cross sections for the scattering of protons from hydrogen and helium are quite different, it is not surprising that the error introduced by these spurious counts was

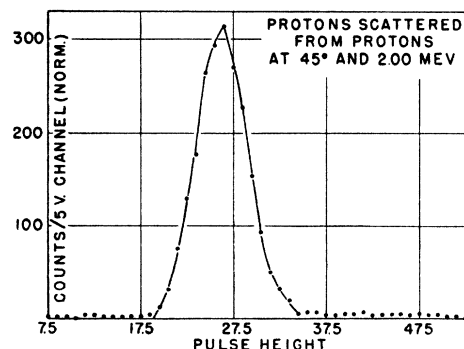


FIG. 4. Pulse-height distribution for protons of 2.00-Mev incident energy scattered at  $45^\circ$  from hydrogen. The number of counts per 5-volt channel has been normalized to unit charge and pressure and plotted at the voltage at the center of the channel.

different for  $p$ -p and  $p$ -He measurements. In the energy range of 2 to 3.5 Mev and the angular range of 45 to 60 degrees the measured  $p$ -p cross sections averaged 3 percent greater than the published values.<sup>2,3</sup> In this same energy and angle range the measured values of the  $p$ -He cross sections were 6 percent higher than those published.<sup>5</sup>

Because of the variation of error with target gas, and because the error introduced by this small chamber increased toward lower scattering angles, it was felt that an attempt to correct  $p$ -t data for measurements at angles below  $40^\circ$  would be unreliable.

## V. CORRECTIONS OF THE DATA

Figure 4 is a plot of the number of pulses per channel *vs* the average pulse height for the protons scattered from protons at  $45^\circ$  and 2 Mev. A tail may be seen extending to the right of the peak. When measurements are made on a two-component gas system at certain angles and energies, the protons scattered from the lighter nuclei will register in the same channels as a portion of the tail from the lower peak. From measurements on pure hydrogen at several appropriate angles and over the energy range of interest here, the con-

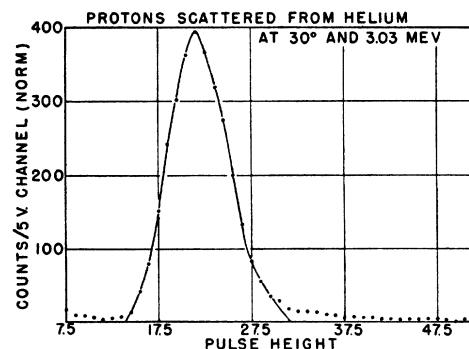


FIG. 5. Pulse-height distribution for protons of 3.03-Mev incident energy scattered at  $30^\circ$  from helium. The number of counts per 5-volt channel has been normalized to unit charge and pressure and plotted at the voltage at the center of the channel.

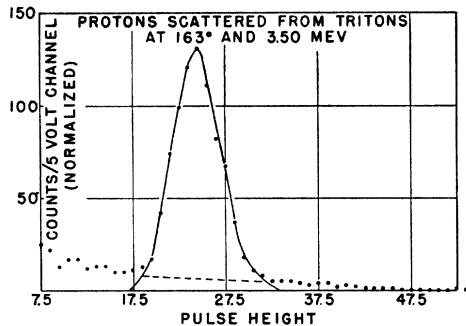


FIG. 6. Pulse-height distribution for protons of 3.50-Mev incident energy scattered at  $163^\circ$  from the tritons in a mixture of tritium and hydrogen. The number of pulses per 5-volt channel has been normalized to unit charge and unit total pressure and plotted at the voltage at the center of the channel.

tribution of the tail of the lower peak to the second peak was determined to be 4.7 percent of the number of counts in the first peak.

As a check on the reliability of the determination of the hydrogen content in a two-component gas target and the reliability of cross-section measurements on the second component using this concentration measurement, a large number of runs were taken on a  $H_2$ -He mixture. The majority of measurements were at 2.5 and 3.0 Mev and  $50^\circ$  and  $55^\circ$  scattering angle. For each run a plot was made of the number of counts per channel per unit pressure and charge vs the channel voltage. Calculations of the hydrogen content of the gas target and the  $p$ -He cross section were made from this graph in the following manner. The sides of the two peaks were extrapolated to zero and the area measured under each peak. Then 4.7 percent of the peak from  $p$ -He scattering was subtracted from the peak caused by  $p$ - $p$  scattering. For the calculation of hydrogen concentration, 97 percent of the remaining number of counts in the second peak were used. This concentration, with the measured pressure, gave the partial helium pressure,

which, with 94 percent of the counts in the first peak, were used to calculate the  $p$ -He cross section. The above treatment of the data gave an average value of the hydrogen concentration, which agreed to within 1 percent of the value determined by mass spectrometer means by Dr. Nier's group. For a given angle and energy of the average  $p$ -He cross section agreed with the value given by Freier, *et al.*, to well within the probable error quoted by then.<sup>5</sup> On the basis of this satisfactory check on the above method of calculating cross section from the data obtained with this small chamber, it was felt that it would be worthwhile to take observations on the cross section for scattering of protons by a gaseous target of tritium contaminated by hydrogen. The data could then be analyzed by using the methods established by the measurements, corrections, and comparisons described above.

All the data taken on the tritium-hydrogen mixture in the angular range of  $40^\circ$  to  $60^\circ$  were treated as described for the hydrogen-helium mixture, except that 97 percent of the counts in the tritium peak were used. It was felt that the behavior of protons scattered from tritium would follow  $p$ - $p$  scattering more closely than  $p$ -He because of the similarity of the coulomb scattering in the two isotopes.

At higher angles, above  $60^\circ$ , the background caused by gamma-rays, machine noise, etc., contributed an appreciable amount to the number of pulses counted. Figure 6 is a plot of a typical pulse-height distribution for protons scattered from tritons at  $163^\circ$  and 3.5 Mev, where the background is highest because of the high energy and the close proximity of the counter to the input window, and slit systems, which are a source of gamma-rays. The general background which extends to either side of the peak has been extrapolated across the bottom of the peak, and this background has been subtracted from the number of pulses in the peak. At these higher angles the number of counts was not corrected

TABLE I. Differential scattering cross section for protons on tritium. The values listed under the laboratory angles are laboratory cross section, those under the center-of-mass angles are center-of-mass cross sections. All cross sections are in units of  $10^{-24}$  cm<sup>2</sup> per unit solid angle.

Lab angle $\theta$ Recoil angle $\phi$ CM angle $\Omega$	41.85		45		50		60		50		71.5		45		90
		54.7		58.6		64.8		76.8		80		90		90	
2.12 Mev			0.270	0.180	0.245	0.170					0.127	0.108			
2.54	0.356	0.232	0.307	0.205	0.269	0.187					0.126	0.107	0.304	0.108	
2.74	0.356	0.232	0.312	0.208	0.281	0.195	0.170	0.129	0.296	0.115	0.120	0.102	0.290	0.103	
3.03	0.368	0.240	0.318	0.212	0.274	0.190	0.186	0.141	0.318	0.124	0.109	0.093	0.274	0.097	
3.25	0.371	0.242	0.328	0.219	0.265	0.184	0.171	0.130	0.296	0.115	0.104	0.089	0.273	0.097	
3.50	0.373	0.243	0.311	0.208	0.266	0.184			0.292	0.114	0.103	0.088	0.238	0.084	
Lab angle $\theta$ Recoil angle $\phi$ CM angle $\Omega$	41.85		90		106.6		27.4		120		140		163		
		96.3		109.5		125		125		136.18		152.4		168.7	
2.12 Mev			0.120	0.127	0.134	0.175	0.627	0.177	0.139	0.213					
2.54	0.302	0.101	0.097	0.103	0.106	0.137	0.500	0.141	0.115	0.176	0.127	0.239			
2.74	0.290	0.098	0.088	0.094	0.107	0.159	0.459	0.129	0.114	0.174	0.116	0.218	0.108	0.241	
3.03	0.274	0.092	0.080	0.085	0.082	0.107	0.376	0.106	0.091	0.140	0.099	0.186	0.099	0.221	
3.25	0.238	0.080	0.071	0.076	0.077	0.099	0.355	0.100	0.088	0.135	0.101	0.190	0.097	0.216	
3.50	0.220	0.074	0.061	0.065	0.070	0.091	0.324	0.091	0.078	0.120	0.085	0.160	0.091	0.203	

downward by 3 percent as was done at the lower angles. Several measurements made on  $p$ -He scattering at high angles, and corrected for background in the manner just described, were in good agreement with the published values.<sup>5</sup>

There are two internal consistency checks on these corrections. First, measurements of the  $p$ - $t$  cross section at a given angle and energy, using targets with widely varying hydrogen impurity, showed no consistent variation with hydrogen contamination. Second, the center-of-mass cross section for the scattering of protons by tritium could be measured for a range of scattering angles by counting the recoil tritons. In the calculation of cross sections from the recoil data obtained from this small chamber, the full number of recoil counts was

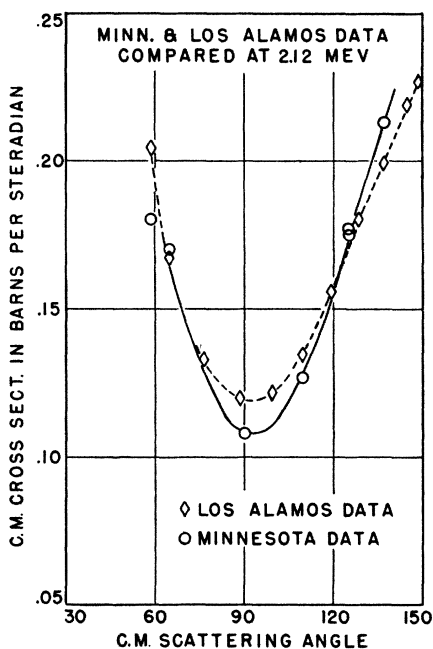


FIG. 7. A comparison of the results obtained at Los Alamos and Minnesota for the center-of-mass cross section at 2.11-Mev incident proton energy.

used. Center-of-mass cross section calculated from observations on the recoil tritons agreed well with those calculated directly from measurements on protons.

#### VI. EXPERIMENTAL RESULTS

All the data have been treated in the manner described in the section on corrections, and cross sections computed according to the formula in Sec. III. The laboratory cross sections for both the scattered protons and recoil tritons, as well as the center-of-mass cross sections calculated from them, are listed in Table I. The probable error estimated for the measurement of charge was  $\pm 1$  percent. The pressure and geometry factor measurements were good to  $\pm \frac{1}{2}$  percent. Other contributions to error in the calculated cross section arose from the measurement of the hydrogen con-

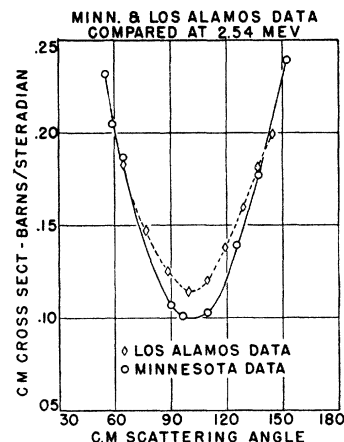


FIG. 8. A comparison of the results obtained at Los Alamos and Minnesota for the center-of-mass cross section at 2.54-Mev incident proton energy.

tamination, estimated to be good to  $\pm 1$  percent, the 3 percent correction for the chamber characteristics, and the correction for background at high scattering angles. For these reasons we have estimated a probable error of  $\pm 5$  percent for the results listed.

Figures 7 and 8 are comparisons of the center-of-mass cross sections obtained in this experiment with those obtained by the Los Alamos group<sup>12</sup> at incident proton energies of 2.11 Mev and 2.54 Mev. The center-of-mass cross section in barns per steradian is plotted against the center-of-mass scattering angle. The agreement between the two sets of data is good at both high and low scattering angles. In the region of minimum cross section, at approximately  $100^\circ$  scattering angle, the results of this experiment are approximately 10 percent lower than those of the earlier experiment. This difference is the sum of the estimated probable errors for the two experiments.

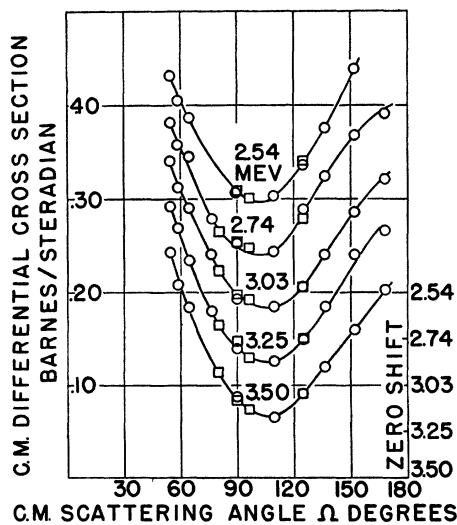


FIG. 9. The center-of-mass cross section in barns per steradian plotted against the center-of-mass scattering angle for the incident proton energies indicated. The cross sections obtained by counting scattered protons are plotted as circles, those from the recoil tritons as squares. The ordinate for each higher curve has been raised by 0.05 barn per steradian. The zeros for the various curves are indicated at the right.

Figure 9 is a plot of the center-of-mass cross section in barns per steradian *vs* the center-of-mass scattering angle for the five highest laboratory energies of incident protons. The cross sections obtained from counting scattered protons are plotted as circles, those from the recoil tritons as squares. The ordinate for each higher curve has been raised by 0.05 barn per steradian in order that the points may be seen more clearly. The scale along the ordinate axis refers to the 3.50-Mev points. The zeros for the points at the lower energies are shown at the right of the graph. The negative curvature at the backward angles in the curve for the 2.74-Mev data is probably not significant.

It is a pleasure to express our appreciation to Professor J. H. Williams for suggesting this problem and

for his advice throughout the course of this work. We should also like to thank the other members of the van de graaff group, Dr. G. R. Keepin, Dr. J. M. Blair, and Messrs. M. Fulk, T. F. Stratton, and J. L. Yarnell for their help in taking data. Mr. Rudolph Thorness made significant contributions to the design of the scattering chamber.

This research was done under the partial support of the Office of Naval Research. It was also materially assisted by the University of Minnesota Technical Research Fund subscribed to by General Mills, Inc., Minneapolis Honeywell Regulator Company, Minneapolis Star Journal and Tribune Company, Minnesota Mining and Manufacturing Company, and Northern States Power Company.

## Stars in Photographic Emulsions Initiated by Protons

LAWRENCE S. GERMAIN

*Radiation Laboratory, Department of Physics, University of California, Berkeley, California, and Reed College, Portland, Oregon*

(Received November 24, 1950)

A study has been made of stars in photographic emulsions initiated by protons from the 184-inch Berkeley cyclotron. Ilford G-5 emulsions were exposed to the deflected proton beam with various Al absorbers interposed to obtain protons of various energies. Both the average number of prongs per star and the cross section for star production were found to increase with increasing proton energy.

### I. INTRODUCTION

A STUDY has been made of stars in photographic emulsions initiated by protons from the 184-inch Berkeley cyclotron. Stars initiated by deuterons have been studied by Gardner and Peterson,<sup>1</sup> while stars initiated by alpha-particles have been studied by Gardner;<sup>2</sup> further work on them is being carried out by Bowker.

### II. PROCEDURE

The present study differs from the previous ones in that electron-sensitive (Ilford G-5) plates were used. If plates of lower sensitivity are used, high energy star prongs will not be seen, and stars containing high energy prongs only will be completely missed. The electron-sensitive plates have the further advantage of

recording the tracks of the high energy protons which initiate the stars. This enables one to find the cross section for star production.

It is desirable to obtain a uniform yet fairly light exposure of the plates. About 20 protons per 100-micron field of view was found to be convenient. Such an exposure could be made by dropping the plates through the deflected proton beam of the 184-proton cyclotron with the emulsion parallel to the beam so that the protons tracks are parallel to the emulsion surface. Although the energy of protons in the deflected beam is about 345 Mev, energies as low as 95 Mev were obtained by placing Al absorbers in front of the plates. The proper thicknesses of Al were calculated from the data on the range of protons in Al given by Smith.<sup>3</sup>

TABLE I. Energy distribution of prongs from stars.

Number of prongs	Energy (Mev)										
	95	115	135	155	175	195	220	245	295	340	
2	18	24	57	43	46	47	55	22	18	34	
3	5	20	27	62	43	41	59	29	30	72	
4	6	4	21	34	32	32	45	33	25	56	
5	2	4	11	18	12	16	28	22	24	50	
6	—	1	2	2	4	2	4	2	6	23	
7	—	—	—	1	—	—	1	4	4	3	
8	—	—	—	—	—	—	—	—	—	2	
Total	31	53	118	160	137	138	191	112	107	240	
Length of track (m)	50.0	60.4	112.3	179.6	144.7	149.0	169.8	90.6	80.6	175.0	

<sup>1</sup> E. Gardner and V. Peterson, *Phys. Rev.* **75**, 364 (1949).

<sup>2</sup> E. Gardner, *Phys. Rev.* **75**, 376 (1949).

<sup>3</sup> J. H. Smith, *Phys. Rev.* **71**, 32 (1947).